Transmission Characteristics of Indoor Infrared Diffuse Links Employing Three-Beam Optical Transmitters and Non-Imaging Receivers

Zan Wang* *Associate Member*, Jae Kyung Pan* *Lifelong Member*

ABSTRACT

Diffuse wireless optical communication offers more robust optical links in terms of coverage and shadowing than line-of-sight links. However, traditional diffuse wireless infrared (IR) transceiver systems are more susceptible to multi-path distortion and great power decrease, which results in limiting high-speed performance. Multi-beam is an effective technique to compensate for multi-path distortion in a wireless infrared environment. The goal of this paper is to analyze the transmission characteristics by replacing traditional diffuse system (TDS) which contains single wide angle transmitter and single element receiver by system consisting of three-beam transmitter and non-imaging receiver (TNS) attached with compound parabolic concentrator (CPC). In the simulation, we use the recursive model developed by Barry and Kahn and build the scenario based on 10 different cases which have been listed in Table 1. Moreover, we also check the reliability of the TNS diffuse link channel by BER test on the basis of different receiver positions and room sizes. The simulation results not only show the basic transmission characteristics of TNS diffuse link, but also are references to design more efficient and reliable indoor infrared transmission systems.

Key Words : Indoor wireless optical communication, Infrared diffuse links, Transmission characteristics

I. INTRODUCTION

The popularity of using convenient wireless communication devices such as laptop computers, office equipments, and personal digital assistants and the fashion of indoor mobile multimedia communication such as voice, data and video, have been prevalent all over the world[1]. This results in growing demands for broadband service and wireless access. As for the wireless communication, the technique for radio frequency (RF) wireless link is developed rapidly and data rate available with RF is also rising[2]. However, compared with wireless optical system RF has many disadvantages such as limited bandwidth, one-mile problem, insecurity, and large spread angle. The drawbacks of RF can be conquered by wireless optical links. Wireless optical link outweighs itself for its flexibility, cost effectiveness, and mobility.

Generally speaking, the wireless optical links can be classified into two types according to distance. They are called long distance systems and short distance systems. The long distance systems are usually employed by outdoor wireless links where the connections between receivers and transmitters are more than 100 meters. The short distance systems are usually used in indoor optical links such as connections in the office and in the personal room (Fig. 1).

The characteristics of indoor wireless optical links would change importantly based on the topology type of channels. As a whole, there are two main channel configurations which are line-

* Department of Electrical Engineering, Chonbuk National University(pan@chonbuk.ac.kr, allen.zanwang@chonbuk.ac.kr)
논문번호 : KICS2008-09-424, 접수일자 : 2008년 9월 29일, 최종논문접수일자 : 2008년 10월 24일

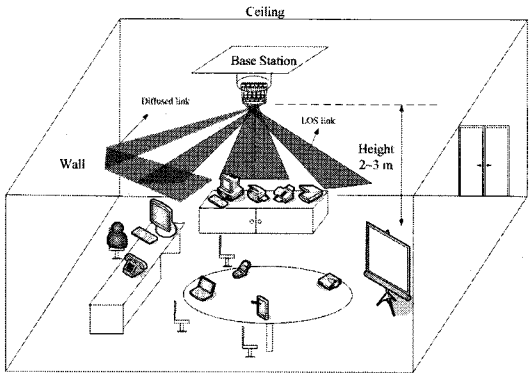

Fig. 1. Demonstration of indoor wireless optical link

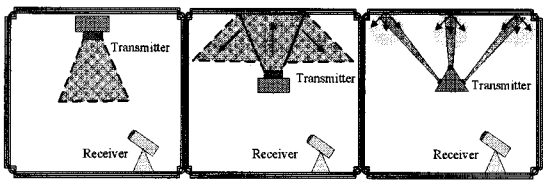

Fig. 2. Wireless optical communication channel configuration

of-sight (LOS) type and diffuse type (Fig. 2). A LOS link is usually used in an ambience where power efficiency and very-high-speed data transmission is required. Nevertheless, Because of its face to face topology, it tends to be blocked. A diffuse link utilizes diffuse reflections from the ceiling or other reflectors. On the other hand, a diffuse link is immune to shading problem and provide wider area of coverage[3].

Here, the analysis is focused on the indoor wireless optical communication. As far as TDS link, the basic performance characteristics have been researched in detail[4]. In this paper, we analyze channel transmission characteristics by proposing an alternative to TDS link based on the employment of TNS link. The basic channel configuration of TNS is shown in Fig. 2 (c). We present simulation results for some channel parameters clearly show the transmission characteristics and performance improvements in terms of impulse response, received power ratio and BER.

This paper is organized as follows: firstly, in section II we discuss simulation model such as transmitter model, receiver model and reflect recursive model for optical power computation in detail. Section III emphasizes TNS diffuse link channel analysis. Here, in order to find the channel transmission characteristics, we build and analyze the scenario based on 10 different situations, then, obtain and plot the BER performances due to different receiver positions and room sizes. Finally, section IV describes the conclusions.

Ⅱ. INDOOR CHANNEL PROPAGATION MODEL

The recursive model for the indoor optical channel developed by Barry and Kahn (1993) is used primarily to find the transmission characteristics. The channel propagation model includes the transmitter model, receiver model and reflect recursive model.

2.1 Transmitter model

Fig. 3 shows the optical transmitter that is modeled as a generalized Lambertian source. The radiant intensity that is a direction at an angle ϕ with the normal of the emitting surface is given by

$$I(\phi) = P_T \frac{n+1}{2\pi} cos^n(\phi) \text{ for } \phi \in \left[-\frac{\pi}{2}, \frac{\pi}{2}\right] \quad (1)$$

$$\text{where } n = \frac{\ln\left(\frac{1}{2}\right)}{\ln[\cos(HPA)]} \quad (2)$$

P_T is the total transmitted power and HPA is the half power angle of the transmitter. n is the mode number of the radiation lobe, which specifies the directionality of the transmitter[5].

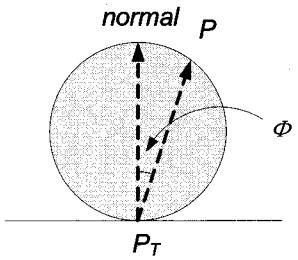

Fig. 3. Transmitter model

Simply, A point transmitter that emits a unit impulse of optical intensity at time zero will be denoted by three parameters: { r_S , $\hat{n}_S$, n} where r_S is its position, $\hat{n}_S$ is the direction vector, and n is the mode number[6].

2.2 Receiver model

Similarly, a receiving element R with position r_R, orientation area A_R, and field of view (FOV) will be denoted by an ordered four-tuple: R={r_R, $\hat{n}_R$, A_R, FOV}. The scalar angle FOV is defined such that a receiver only detects light whose angle of incidence (with respect to the detector normal $\hat{n}_R$) is less than FOV (Fig. 4). A limited field of view may be an inadvertent effect of detector packaging, or it may be used intentionally to reduce unwanted reflections or noise[6].

The receiver uses an ideal optical concentrator[7], which provides gain at the expense of a narrow FOV. The effective area at the angle α of an optical detector of area A_{det} with an ideal optical concentrator of reflective index N and cutoff angle α_c is given by

$$A(\theta)=\frac{N^2 A_{\det}}{\sin^2(\alpha_c)}\cos(\alpha)rect(\alpha,\alpha_c) \qquad (3)$$

One implementation of a nearly ideal optical concentrator is a CPC, which provides an effective area at an angle α that is well modeled by equation[8]:

$$A(\theta)=\frac{N^2 A_{\det}}{\sin^2(\alpha_c)}\frac{\cos(\alpha)T}{1+(\alpha/\alpha_c)^{2R}} \qquad (4)$$

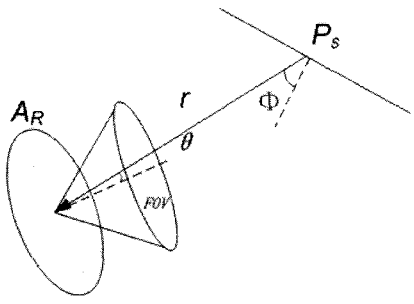

Fig. 4. Receiver model

2.3 Reflect recursive model

Fig. 5 shows the reflect recursive model. Considering that surfaces are completely irregular and reflect infrared signal without privileging any particular direction. These surfaces look equally bright when observed from different directions. The reflection patterns of these surfaces are completely diffuse and can be correctly approximated using Lambertian model. In the model, the differential reflectors are seen as the transmitters. The receiver is characterized by its FOV. The reflector model considers that all the surfaces are Lambertian reflectors. It means that the reflected signal is independent from the incident signal. So, the channel transfer function could be expressed as follows

$$h(t)=\frac{n+1}{2\pi}\cos^n(\phi)\cos(\theta)\frac{A_R}{R^2}\delta\left[t-\frac{R}{c}\right] \qquad (5)$$

where R is the distance between transmitter and receiver. A_R is the detector size. n is the mode number.

The received signal is then a delayed $\delta(t)$ function, the delay is proportional to the distance R and the light speed c. For the bounces after the first reflection, we use the recursive model proposed by Barry[6]:

$$h^k(t)=\frac{n+1}{2\pi}\sum_{i=1}^{n}\frac{\rho_j\cos^n(\phi)\cos(\theta)}{R^2}h^{k-1}(t) \qquad (6)$$

where ρ_j is the reflectivity coefficient of the cell.

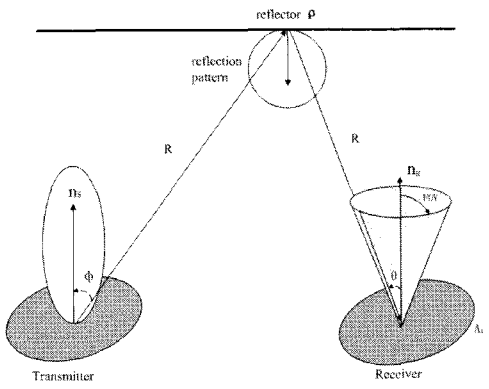

Fig. 5. Reflect recursive model

Ⅲ. TRANSMISSION CHARACTERISTICS EVALUATION

In this section, the transmission characteristics of the channel formed by a three-beam transmitter and non-imagining receiver are considered. The transmitted signal propagates to the receiver through multiple reflections from room surfaces. Propagation simulations were carried out in an empty room with floor dimensions of 8 m × 6 m (length × width), and ceiling height of 3 m. Up to the third order reflections were taken into account. Walls (including ceiling) and floor were modeled as Lambertian reflectors with reflection coefficients 0.6 and 0.3 (Table 1) respectively. Reflections from doors and windows are considered completely the same as reflections from walls.

Fig. 6 shows the scenario of non-directed diffuse optical wireless communication system with proposed TNS link. The transmitter and the receiver are assumed to be put on the same transmission platform of the room, whose height is

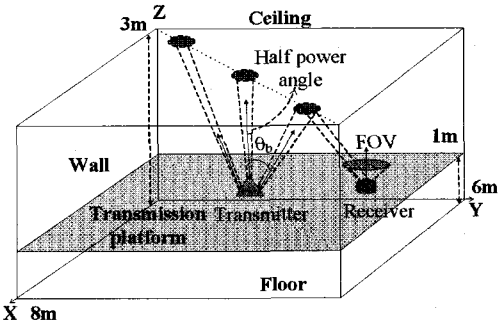

Fig. 6. Scenario of non-directed diffuse optical wireless communication system with proposed TNS link

1 m. The transmitter has one optical beam pointing the ceiling vertically and two optical beams arranged with uniformly distributed angle. Therefore the transmitter has 3 beams. Total radiating power is 1 W which is the sum of three optical beams. Angle θ_b formed by direction vector of two adjacent beams is 60 degree. Although the transmitter can take other forms, we use the form described here because of possibility of realization and simplicity of analysis. As the Table 1 shown, these parameters list in it dominate transmission characteristics of TDS

Table 1. Parameters for evaluation

Parameters	Evaluation 1	Evaluation 2	Evaluation 3	Evaluation 4	Evaluation 5	Evaluation 6	Evaluation 7	Evaluation 8	Evaluation 9	Evaluation 10
Room Dimensions	(8m, 6m, 3m)	(8m, 6m, 3m)	(8m, 6m, 3m)	(8m, 6m, 3m)	(8m, 6m, 3m)	(8m, 6m, 3m)	(8m, 6m, 3m)	(8m, 6m, 3m)	(8m, 6m, 3m)	Change
Reflection Coefficients										
Walls	0.7	Change	0.6	0.6	0.6	0.6	0.6	0.6	0.6	0.6
Ceiling	0.7	Change	0.6	0.6	0.6	0.6	0.6	0.6	0.6	0.6
Floor	0.3	0.3	0.3	0.3	0.3	0.3	0.3	0.3	0.3	0.3
Transmitter										
Locations	(4m,3m, 1m)	(4m, 3m, 1m)	(4m, 3m, 1m)	Change	(4m, 3m, 1m)	(4m, 3m, 1m)	(4m, 3m, 1m)	(4m, 3m, 1m)	(4m, 3m, 1m)	(4m, 3m, 1m)
Branches	3	3	3	3	3	3	3	3	3	3
HPSA	15°	15°	Change	15°	15°	15°	15°	15°	15°	15°
Elevation	90°	90°	90°	90°	90°	90°	90°	90°	90°	90°
Azimuth	37°	37°	37°	37°	Change	37°	37°	37°	37°	37°
Receiver										
Locations	(0.5m, 0.5m, 1m)	(3.7m, 2.7m, 1m)	(3.7m, 2.7m, 1m)	(3.7m, 2.7m, 1m)	(3.7m, 2.7m, 1m)	(change, change, 1m)	(3.7m, 2.7m, 1m)	(3.7m, 2.7m, 1m)	(3m, 3m, change)	(3.7m, 2.7m, 1m)
Area	1 cm²	1 cm²	1 cm²	1 cm²	1 cm²	1 cm²	1 cm²	1 cm²	1 cm²	1 cm²
FOV	85°	85°	85°	85°	85°	85°	Change	85°	85°	85°
Elevation	90°	90°	90°	90°	90°	90°	90°	Change	90°	90°
Azimuth	0°	0°	0°	0°	0°	0°	0°	0°	0°	0°

diffuse link-based channel. The receiver has only one photo detector pointing at the ceiling vertically with CPC, and its receiving area is 1 cm^2. Each optical beam of the transmitter is diffusively reflected at a surface (spot area) and the distribution of reflected power of optical beam has its peak in each spot area. As the transmitter has 3 beams, the number of spots is 3. If any spot area is included in receiver's *FOV*, the receiver can receive diffusively reflected signal. In the following analysis, in order to simplify the analysis, we only consider transmitter with three beams and single non-imaging receiver.

3.1 Scenario performances evaluation

Here, in order to understand the behavior of TNS link, we investigate the performance of TNS in terms of ten evaluations in Table 1. Additionally, BER test simulation is carried out to check the reliability of TNS link compared with TDS in an AWGN channel.

In evaluation 1, for comparison purposes, a TDS link has been simulated to generate channel impulse responses. Here, the receiver points straight up and its position is chosen at the room corner (x = 0.5 m, y = 0.5 m, z= 1 m). Since the transmitter is usually placed in the center of the room, this is to examine the worst receiver position case. Because the distance between the transmitter and the receiver becomes large, the power of the collected optical signal decreases.

In contrast to the traditional diffuse link, from Fig. 7, it is clearly seen that the TNS structures are better than TDS. This is due to the fact that the impulse response of these configurations contains more peaks corresponding to the direct LOS components between the diffusing spots and the receiver. Furthermore, the impulse response results have further confirmed the findings that most of the collected signal is in the first-order reflection, concentrated within a very short time period due to the contribution of the many direct LOS components.

Consider the scenario in the second column of Table 1, entitled evaluation 2. Unlike evaluation 1, the transmitter and receiver both have been moved in the center of the room. In order to evaluate the effect of reflection coefficients, we refer to nine reflection coefficients from 0.05 to 0.8. Fig. 8 compares the performance of TNS diffuse link and TDS link. The curves in the figure show that the received power ratios become larger with the increase of reflection coefficient values. It is easy to understand that higher reflection coefficient value means less optical power is absorbed by the reflector in the reflection. Compared with results obtained by employing TDS link, the received power ratio of TNS is at least 60 dB better.

In the case of Evaluation 3, to show how *HPA* affect power ratios, performances of TNS link have been simulated on condition of different *HPA*. The power ratio as a function of the *HPA* is depicted in Fig. 9, which shows that when the *HPA* is around 10°, the received power ratio is the largest. However, after 15° the received power

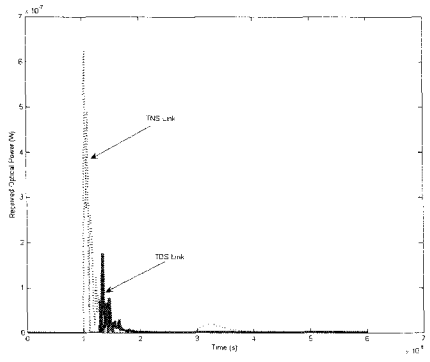

Fig. 7. Impulse response of TNS Link

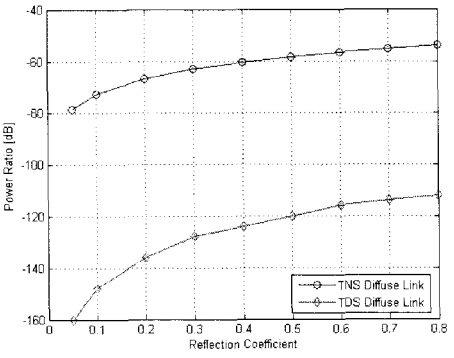

Fig. 8. Evaluation of power ratio based on different reflection coefficients

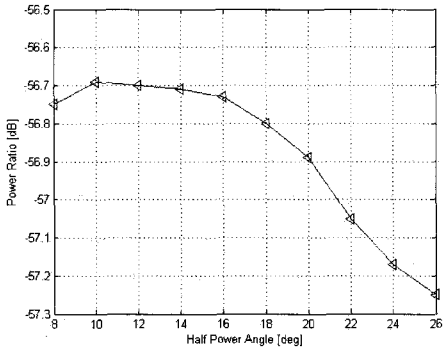

Fig. 9. Evaluation of power ratio based on different half power semi-angles

ratios decrease rapidly with the increase of *HPA*. The reason is that when *HPA* is larger than 15 degree, incident angles of some reflected beams are bigger than receiver cutoff angle, and some beams experienced more than one reflection order which greatly decreases the optical power.

In Evaluation 4, in order to cover more possible channel characteristics of proposed TNS diffuse link, the transmitter is placed at various locations along the two diagonals of the room on the platform as listed in Table 2. For each transmitter movement, simulation computations are carried out when receiver position is in center of the transmission platform. Observing Table 2, we find that the power is greatly decreased in positions near the corner ((x, y, z) = (5.5 m, 1.5 m, 1 m) and (2.5 m, 4 m, 1 m)), compared with other positions. This is owing to two factors, the peak correspondences are decreased since more optical beams experiences multi-reflection from the floor and walls when the transmitter approaches the corner and the distance between transmitter and receiver is larger. Especially in the position (5.5 m, 1.5 m, 1 m), where two side beam spots on the ceiling is very close to the side walls oriented at right angles with each other, which leads to a great power decrease to the transmission channel. In the situation here, the strongest power ratio could be obtained when transmitter position is in the center of the room.

As for evaluation 5, to simulate the TNS diffuse link under the azimuth angel effect, the transmitter is placed at different azimuth angles. The azimuth angle at position r is defined as the angle between $\hat{x}$ and the projection of r onto the x-y plane, with a sign defined so that $\hat{y}$ has an azimuth of 90°. The simulations are carried out when the transmitter azimuth angle is fixed at values labeled on x axis shown in Fig. 10 respectively. Moreover, Fig. 10 shows that the strongest power ratios are obtained with an azimuth angle between 30° and 50° and the weakest ones are found at 0° and 90°. This is due to the fact that two side beam spots become closer to two opposite side walls with transmitter azimuth angle at 0° and 90°. It results in high order multi-reflection correspondences in contrast to other cases. Therefore, the received power ratios are greatly decreased.

In comparison with preceding evaluations, where a receiver in center is employed, in evaluation 6

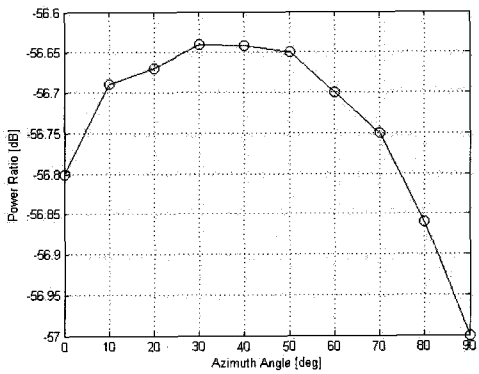

Fig. 10. Evaluation of power ratio based on different azimuth angles

Table 2. Simulation results of evaluation 4

Parameters	Source Position (x, y, z)						
	(2, 1.5, 1)	(4, 2.5, 1)	(6, 4, 1)	(5.5, 1.5, 1)	(5, 2, 1)	(3, 3.5, 1)	(2.5, 4, 1)
Power Ratio (dB)	-56.6282	-55.8343	-58.6748	-61.934	-60.025	-56.9289	-59.9259

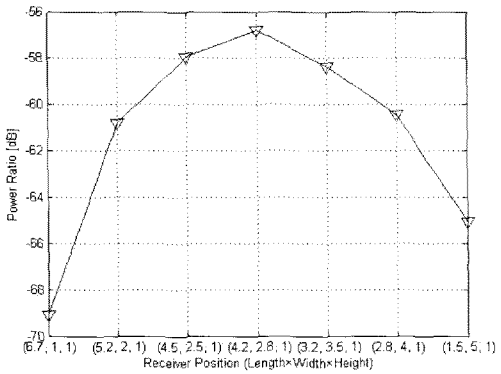

Fig. 11. Evaluation of power ratio based on different receiver positions

the receiver place is altered. Fig. 11 represents the simulation results as a function of the spatial arrangement of receiver locations which are chosen along one diagonal of the room. Fig. 11 also shows the largest received power ratio is obtained as the receiver is fixed in the center.

As shown in Fig. 12, for evaluation 7, in order to investigate the effect of *FOV* of the non-imagining receiver on the performances of TNS diffuse link, the *FOV* of the receiver is increased from 20° to 90°. The system performances are evaluated for the case when the transmitter is at the center of the transmission platform. The results show an increase in received power ratio with large field of view.

Evaluation 8, similar to evaluation 7, is an investigation of receiver angle with the transmitter mounted in the center of the room on the

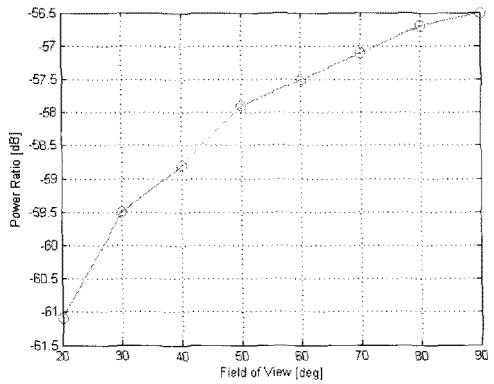

Fig. 12. Evaluation of power ratio based on different field of view

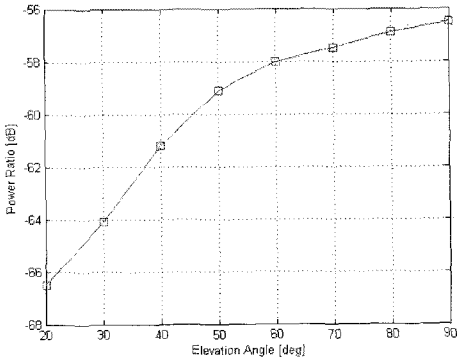

Fig. 13. Evaluation of power ratio based on different elevation angle

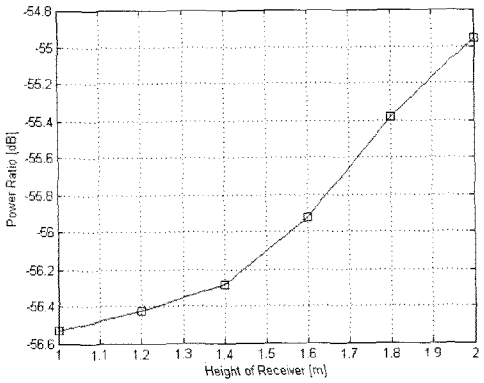

Fig. 14. Evaluation of power ratio based on different height of receiver

transmission platform. Nevertheless, the receiver is pointed not always straight up owing to various elevation angles from 20° to 90°. Fig. 13 presents curves of received power ratio vs. elevation angle. The figure clearly demonstrates that increasing the elevation angle within 90° improves received power ratio.

In contrast to the evaluations considered so far, evaluation 9 and evaluation 10 of the ninth and tenth column of the Table 1, represent TNS diffuse links, with the transmitter in the center of the room, 1 m above the floor, and aimed towards the ceiling, but different receiver height and room size. It is found that, in Fig. 14 which plots the simulation results, the higher receiver positions offer better received power ratios, since higher positions are closer to the beam spots on the ceiling which contains more peaks corresponding. In order to observe the influences of room size on

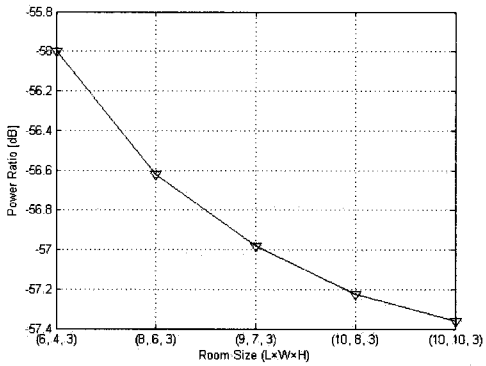

Fig. 15. Evaluation of power ratio based on different room size

performance of TNS diffuse link, in evaluation 10, the room sizes are fixed as (x, y, z) = (6 m, 4 m, 3 m), (8 m, 6m, 3m), (9 m, 7m, 3m), (10 m, 8m, 3m) and (10, 10, 3) respectively. The received power ratio over the room size is illustrated in Fig. 15. Simulation results show that the smaller the room size is, the bigger the power ratio becomes.

3.2 Error estimation

In order to evaluate the reliability of TNS diffuse link compared with TDS link, we evaluate the BER using binary pulse position modulation (BPPM) which is an orthogonal modulation scheme offering a decrease in average power requirement to achieve a desired BER compared with on-off keying (OOK). The measurements encompass the comparison between TDS link and TNS link. The simulations are conducted in an AWGN channel. The probability of a symbol error could be calculated by equations which are derived from Barry[6]:

$$P_r[symbol\ error] = 1 - P_r[correct\ symbol] \quad (7)$$
$$= (L-1)E\left\{Q\left(\frac{S+n}{\sqrt{N_0}}\right)\right\}$$

$$Bit\ Error\ Rate = \frac{L/2}{L-1}P_r[symbol\ error] \quad (8)$$
$$\approx Q\left(\frac{S}{\sqrt{2N_0}}\right)$$

where, noises n are Gaussian random variables with zero mean and variance N_0, L is the level of pulse-position modulation, $(L/2)/(L\text{-}1)$ represents the average number of bit errors per symbol error.

In the simulation, the transmitter has been located in the center of the room. We choose positions (5.2 m, 2 m, 1m), (4.5 m, 2.5 m, 1 m) and (4.2 m, 2.8 m, 1 m) of evaluation 6 as the locations of receiver. Furthermore, calculations are considered under the constraints of background noise (AWGN channel). The BER performances are obtained based on these different receiver positions respectively. Simulation results shown in Fig. 16 quoted for TNS diffuse link versus those obtained with a TDS link. Fig. 16 also shows that in both cases when the receiver position is near the center (4.2 m, 2.8 m, 1 m), the BER is the best. This is attributed to the fact that the distance between the transmitter and receiver is minimum compared to other locations, resulting in a strong received signal power. Besides, it is seen that the use of TNS link produces enhancement in the performance of the signal-to-noise ratio (SNR), since TNS reaches the same BER levels with lower SNR levels than TDS link. For instance, we note that in the position near the center (4.2 m, 2.8 m, 1 m), to achieve the same BER level of 10^{-5}, TNS diffuse link performs about 2.7 dB better than TDS link. Therefore, in contrast to TDS diffuse link, obviously, TNS link is more efficient.

In comparing to the optical power efficiency of TDS diffuse link in transmission at a given room size ((6 m, 4 m, 3m), (8 m, 6 m, 3 m), (9 m, 7 m, 3 m) respectively), we compare the SNR required to achieve at the same BER employing BPPM modulation scheme through an AWGN channel. The simulation results plotted in Fig. 17 present the BER as a function of SNR per bit, E_b/N_0. Note that the smaller the room size is, the better the BER performances are obtained. This is due to small room size could lower the reflection order of beams reaching the detector, in other words, small room size decreases the optical path loss. The simulation results of TDS link are also illustrated in Fig. 17 for comparison purposes. The curves of TNS link and TDS link in the same situation are in stark contrast. Similarly, as

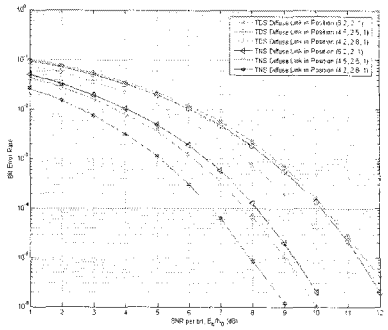

Fig. 16. Simulation results of BER based on different receiver position

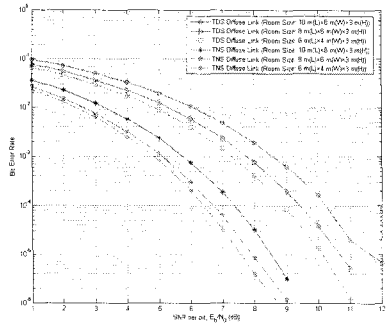

Fig. 17. Simulation results of BER based on different room size

compare to TDS link on the AWGN channel at 10^{-5} BER, we find that the SNR gains of TNS diffuse link versus TDS, in order of room size such as (6 m, 4 m, 3 m), (8 m, 6 m, 3 m) and (9 m, 7 m, 3 m), are 2.6 dB, 2.8 dB and 3.1 dB respectively. Obviously, TNS has absolute advantages in optical power efficiency.

Ⅳ. CONCLUSION

In this paper, the channel transmission characteristics of three-beam transmitters and non-imaging receivers attached with CPC are analyzed by evaluating the channel performances on the basis of 10 different situations (Table 1) and BER test based on varied receiver position and room size.

In conclusion, numerical results obtained through considering various parameters have very clearly shown the basic transmission characteristics of TNS link. Moreover, while keeping the total power constant, a remarkable performance improvement is achieved by employing TNS diffuse link over TDS link. In the meanwhile, through the simulation results, we have found that the impulse response has significantly increased compared to the TDS link (Evaluation 1). This is due to two major factors: the contributions of the diffusing spots produced by a three-beam transmitter and the use of a CPC attached non-imaging receiver. When received power ratio is calculated by considering nine reflection coefficients from 0.05 to 0.8 (Evaluation 2), we note that the received power ratio of TNS is at least 60 dB better than TDS. Additionally, in the error estimation, in the position near the room center (4.2 m, 2.8 m, 1 m), to achieve the same BER level of 10^{-5}, TNS diffuse link performs about 2.7 dB better than TDS link. Also, in contrast to TDS link at 10^{-5} BER on the AWGN channel, we find that the SNR gains of TNS diffuse link versus TDS, in order of room size such as (6 m,4 m,3 m), (8 m, 6 m, 3 m) and (9 m, 7 m, 3 m), are 2.6 dB, 2.8 dB and 3.1 dB respectively. The results described in this paper not only show the transmission performances of TNS link, but also are valuable references to design more efficient and reliable indoor infrared transmission systems.

References

[1] M. J. McCullagh and D. R. Wisely, "155Mbit/s optical wireless link using a bootstrapped silicon APD receiver," *Electronics Letters*, Vol.30, No.5, pp.430-432, Mar. 1994.

[2] Chaturi Singh, Joseph John, Y. N. Singh, and K. K. Tripathi, "Design Aspects of High-Performance Indoor Optical Wireless Transceivers," *ICPWC IEEE*, pp.14-18, Jan. 2001.

[3] A. Mahdy and J. Deogun, "Wireless Optical Communications: A Survey," *IEEE WCNC*, pp. 2399-2404, Mar. 2004.

[4] Chuan Peng, Zan Wang, Ji Do Kim, and Jae

Kyung Pan, "Channel Characteristics of Indoor Wireless Infrared Communication System Due to Different Transceiver Conditions," *Journal of KICS*, Vol.33, No.2, pp.198-203, Feb. 2008.

[5] Rui T. Valadas, Antonio R. Tavares, and A. M. De Oliveira Duarte, "Angle Diversity to Combat the Ambient Noise in Indoor Optical Wireless Communication Systems," *International Journal of Wireless Information Networks*, Vol.4, No.4, 1997.

[6] J. Barry, *Wireless Infrared Communications*, Kluwer Academic Publishers, 1994.

[7] W. Welford and R. Winstion, *High Collection Nonimaging Optics*, New York: Academic, 1989.

[8] K. -P. Ho and J. M Kahn, "Compound Parabolic Concentrators for Narrow-band Wireless Infrared Receivers," *Opt. Eng.*, Vol.34, pp.1385-1395, May 1995.

왕 잔 (Zan Wang) 준회원

2005년 7월 Changchun Univ. of Science and Technology Biomedical Engineering 졸업
2006년 9월~현재 전북대학교 대학원 전기공학과 석사과정
<관심분야> 실내무선광통신, 광통신 시스템

반 재 경 (Jae Kyung Pan) 종신회원

1980년 2월 연세대학교 전자공학과 졸업
1982년 2월 연세대학교 대학원 전자공학과 졸업(공학석사)
1987년 8월 연세대학교 대학원 전자공학과 졸업(공학박사)
1987년 5월~현재 전북대학교 전자정보공학부 교수
<관심분야> 실내무선광통신, 광통신 소자 및 시스템